SPACE RADIATION LABORATORY

CALIFORNIA INSTITUTE OF TECHNOLOGY
Pasadena, California 91125

SEMI-ANNUAL STATUS REPORT

for

NATIONAL AERONAUTICS AND SPACE ADMINISTRATION
Grant NGR 05-002-160*
"RESEARCH IN PARTICLES AND FIELDS"

for

1 April 1982 - 31 March 1983

R. E. Vogt, Principal Investigator
A. Buffington, Coinvestigator
L. Davis, Jr., Coinvestigator
E. C. Stone, Coinvestigator

*NASA Technical Officer: Dr. A. G. Opp, Physics and Astronomy Programs

particle populations. The large scale radial gradients for the anomalous oxygen and the >75 MeV protons have been previously reported by others for the 1 - 20 AU range by comparing the intensities at the Pioneer spacecraft to those near Earth. By using the separation of the two Voyager spacecraft we can determine the local radial gradients during the time intervals of the variations and compare these to the large scale gradients. In the 1978 period the spacecraft are ~4 AU from the Sun and ~0.3 AU apart. In 1980 they have moved out to an average radial position of ~7.2 AU and have moved apart ~ 1.25 AU. They are well aligned in both longitude and latitude. During the 1978 and 1980 time intervals Voyager 1 is always farther from the Sun than Voyager 2; thus for positive radial gradients Voyager 1 will measure a higher intensity than Voyager 2.

Figure 2

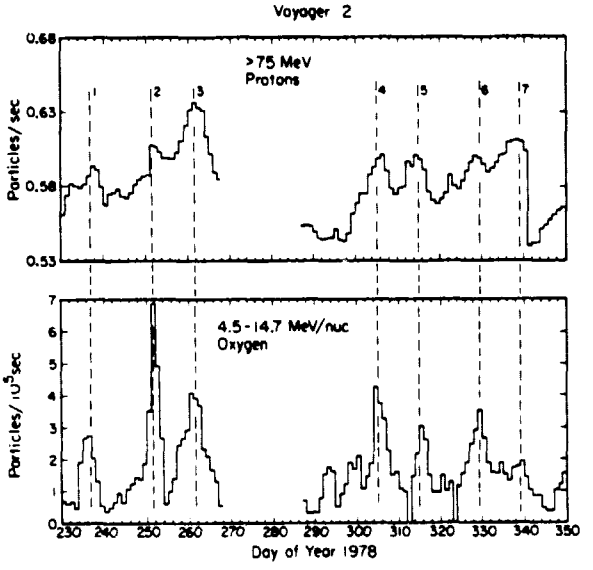

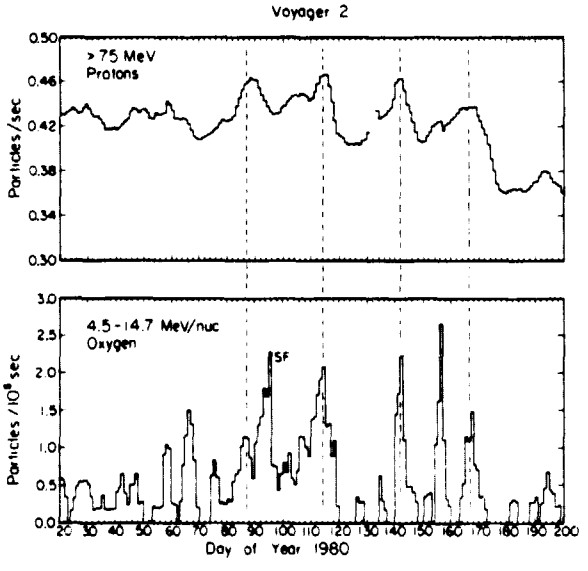

Figure 3

SEMI-ANNUAL STATUS REPORT

NASA Grant NGR 05-002-160

Space Radiation Laboratory (SRL)
California Institute of Technology

1 April 1982 - 31 March 1983

This report covers the research activities in Cosmic Rays, Gamma Rays, and Astrophysical Plasmas supported under NASA Grant NGR 05-002-160. The report is divided into sections which describe the activities, followed by a bibliography.

This group's research program is directed toward the investigation of the astrophysical aspects of cosmic radiation and of the radiation and electromagnetic field environment of the Earth and other planets. We carry out these investigations by means of energetic particle and photon detector systems flown on spacecraft and balloons.

1. Cosmic Rays and Astrophysical Plasmas

This research program is directed toward the investigation of galactic, solar, interplanetary, and planetary energetic particles and plasmas. The emphasis is on precision measurements with high resolution in charge, mass, and energy. The main efforts of this group, which are supported partially or fully by this grant, have been directed toward the following two categories of experiments.

1.1. Activities in Support of or in Preparation for Spacecraft Experiments

These activities generally embrace prototypes of experiments on existing or future NASA spacecraft or they complement and/or support such observations.

1.1.1. The High Energy Isotope Spectrometer Telescope (HEIST II)

HEIST-II is a large area (0.25 m^2sr) balloon borne isotope spectrometer designed to make high-resolution measurements of isotopes in the element range from neon to nickel ($10 \leq Z \leq 28$) at energies of about 3 GeV/nucleon. The instrument, shown schematically in Figure 1, consists of a stack of 12 NaI(Tl) scintillators, two Cerenkov counters, and two plastic scintillators. Each of the 2-cm thick NaI disks is viewed by six 1.5-inch photomultipliers whose combined outputs measure the energy deposition in that layer. In addition, the six outputs from each disk are compared to determine the position at which incident nuclei traverse each layer to an accuracy of ~2 mm. The Cerenkov counters, which measure velocity, are each viewed by twelve 5-inch photomultipliers using light integration boxes.

HEIST-II determines the mass of individual nuclei by measuring both the change in the Lorentz factor ($\Delta\gamma$) that results from traversing the NaI stack, and the energy loss (ΔE) in the stack. Since the total energy of an isotope is given by $E = \gamma M$ the

mass M can be determined by $M = \Delta E/\Delta\gamma$. The instrument is designed to achieve a typical mass resolution of 0.2 amu.

The HEIST II system integration was brought nearly to a conclusion during the past year, and a calibration on ^{56}Mn ions was carried out at the Berkeley Bevalac. The calibration included a newly-assembled aerogel mosaic with index of refraction $n \approx 1.1$. A fly-cutting technique allowed preparation of the aerogel blocks within 50μ of the desired size. Forty eight blocks are assembled in the mosaic to make a Cerenkov radiator 6 cm thick and nearly 60 cm in diameter. The detector signal is 23±4 photoelectrons for the passage of a relativistic muon. This number is adequate to achieve a resolution of 0.2 amu.

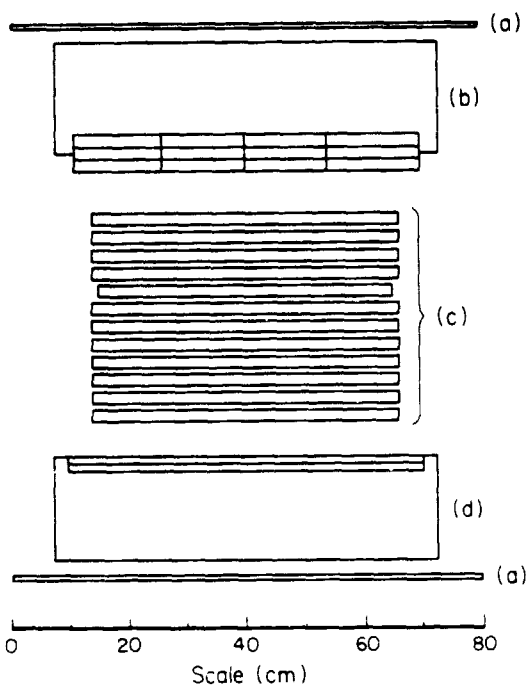

Figure 1. Schematic diagram of the experimental apparatus. (a) plastic scintillators; (b) aerogel Cerenkov counter; (c) NaI scintillator stack; (d) bottom Cerenkov counter with Pilot 425 and teflon. Large rectangles show Cerenkov light collection boxes.

The Bevalac calibration also provided the first major operation of our new data recording system which utilizes commercial video recorders. The system performed satisfactorily, and an efficient off-line conversion to normal computer magnetic tape has been achieved.

Preliminary analysis of the Bevalac data has indicated that the macroscopic index of refraction variation of the mosaic blocks is below 0.003. The variation gradient is sufficiently small that the experiment position-measuring specification, ±2 mm, is adequate for correcting Cerenkov counter response variation with position over approximately 75% of the aerogel area. The aerogel microscopic index of refraction variation is measured at about ±0.00025, integrated over the path of the

particles through the 6 cm of radiator. This produces typically 0.1 a.m.u. of systematic mass error for Mn ions, just acceptable for the experiment. Scintillation in the aerogel, which might degrade the mass resolution near the aerogel threshold, is demonstrated to be less than a negligible 1%.

The NaI scintillator stack also received its first exposure to ions heavier than argon. The ^{56}Mn penetrated to the final NaI layer, and data with the apparatus translated in (x,y) provided coverage for a response map. The NaI stack was able to measure the energy of the stopping ^{56}Mn ions to an accuracy of 0.2% or better, as expected, and the position resolution for these ions was ±1.3 mm. Systematic contributions to error in the position measurement were less than 1 mm.

During the coming year, we expect to continue with analysis of the Bevalac data, generating response maps for the detectors, and further understanding the details of instrument response. We expect to fly HEIST II from Palestine, Texas, during the September 1983 high altitude wind turnaround.

1.2. Experiments on NASA Spacecraft

The SR&T grant program of the Space Radiation Laboratory is strengthened by and contributes to the other programs described here. Activities related to these programs are primarily funded by mission-related contracts but grant funds are used to provide a general support base and the facilities which make these programs possible.

1.2.1. An Electron/Isotope Spectrometer (EIS) Launched on IMP-7 on 22 September 1972 and on IMP-8 on 26 October 1973

This experiment is designed to measure the energy spectra of electrons and positrons (0.16 to ~6 MeV), and the differential energy spectra of the nuclear isotopes of hydrogen, helium, lithium, and beryllium (~2 to ~50 MeV/nucleon). In addition, it provides measurements of the fluxes of the isotopes of carbon, nitrogen, and oxygen from ~5 to ~15 MeV/nucleon. The measurements from this experiment support studies of the origin, propagation, and solar modulation of galactic cosmic rays; the acceleration and propagation of solar flare particles; and the origin and transport of energetic magnetospheric particles observed in the plasma sheet, adjacent to the magnetopause, and upstream of the bow shock.

The extensive EIS data set has been utilized in comprehensive studies of solar, interplanetary, and magnetospheric processes. Correlative studies have involved data from other IMP investigations and from other spacecraft, as well as direct comparisons of EIS data from IMP-7 and IMP-8. These studies have resulted in the following recent talks and papers:

- "Plasma Behavior During Energetic Electrons Streaming Events: Further Evidence for Substorm Associated Magnetic Reconnection," J. W. Bieber et al., *Geophys. Res. Ltrs.* 9, 664-667 (1982).

- "Reconnection - Associated Energization of Plasma Sheet Electrons," J. W. Bieber et al., *EOS Trans. AGU* 63, 418 (1982).

- "Microstructure of Magnetic Reconnection in Earth's Magnetotail," J. W. Bieber et al., *J. Geophys. Res.* (1983 in press).

1.2.2. An Interstellar Cosmic Ray and Planetary Magnetospheres Experiment for the Voyager Missions Launched in 1977.

This experiment is conducted by this group in collaboration with F. B. McDonald, J. H. Trainor, and A. W. Schardt (Goddard Space Flight Center), W. R. Webber (University of New Hampshire), and J. R. Jokipii (University of Arizona), and has been designated the Cosmic Ray Subsystem (CRS) for the Voyager Missions. The experiment is designed to measure the energy spectra, elemental and (for lighter elements) isotopic composition, and streaming patterns of cosmic-ray nuclei from H to Fe over an energy range of 0.5 to 500 MeV/nucleon and the energy spectra of electrons with 3 - 100 MeV. These measurements will be of particular importance to studies of stellar nucleosynthesis, and of the origin, acceleration, and interstellar propagation of cosmic rays. Measurements of the energy spectra and composition of energetic particles trapped in the magnetospheres of the outer planets are used to study their origin and relationship to other physical phenomena and parameters of those planets. Measurements of the intensity and directional characteristics of solar and galactic energetic particles as a function of the heliocentric distance will be used for *in situ* studies of the interplanetary medium and its boundary with the interstellar medium. Measurements of solar energetic particles are crucial to understanding solar composition and solar acceleration processes.

The CRS flight units on both Voyager spacecraft have been operating successfully since the launches on August 20, 1977 and September 5, 1977. The CRS team participated in the Voyager 1 and 2 Jupiter encounter operations in March and July 1979, and in the Voyager 1 and 2 Saturn encounters in November 1980 and August 1981. The Voyager data represent an immense and diverse data base, and a number of scientific problems are under analysis. These investigation topics range from the study of galactic particles to particle acceleration phenomena in the interplanetary medium, to plasma/field energetic particle interactions, to acceleration processes on the sun, to studies of elemental abundances of solar, planetary, interplanetary, and galactic energetic particles, and to studies of particle/field/satellite interactions in the magnetospheres of Jupiter and Saturn.

The following publications and papers for scientific meetings, based on Voyager data, were generated:

- "The Voyager Encounter with Uranus," E. C. Stone, 275-291 in *Uranus and the Outer Planets*, ed. G. Hunt, Cambridge University Press, Cambridge, England (1982).

- "An Analysis of the Structure of Saturn's Magnetic Field Using Charged Particle Absorption Signatures," D. L. Chenette and L. Davis, Jr., *J. Geophys. Res.* 87, 5267-5274 (1982).

- "An Analysis of the Structure of Saturn's Magnetic Field Using Charged Particle Absorption Signatures," D. L. Chenette and L. Davis, Jr., Talk presented at Tucson Saturn Conference, 1982, Tucson, Arizona.

- "The Companions of Mimas: Charged Particle Absorption Signatures and a Comparison with Recent Imaging Discoveries.," D. L. Chenette et al., Talk given at Tucson Saturn Conference, 1982, Tucson, Arizona.

- "Voyager Observations of Saturn's Rings: An Overview," E. C. Stone, Invited talk presented at I.A.U, Colloquium No. 75, Toulouse, France.

- "Voyager Observations of the Uranian Rings: A Preview," E. C. Stone, Invited talk presented at I.A.U, Colloquium No. 75, Toulouse, France.

- "The Voyager Encounters with Saturn," E. C. Stone, *AIAA* (1983 submitted).

- "Energetic Oxygen and Sulfur in the Jovian Magnetosphere and Their Contribution to the Auroral Excitation," N. Gehrels and E. C. Stone, *J. Geophys. Res.* (1982 submitted).

- "The Mimas Ghost Revisited: An Analysis of the Electron Flux and Electron Microsignatures Observed in the Vicinity of Mimas at Saturn," D. L. Chenette and E. C. Stone, *J. Geophys. Res.* (1982 submitted).

- "Temporal Variations of the Anomalous Oxygen Component," A. C. Cummings and W. R. Webber, Solar Wind 5 conference (1982).

- "Voyager Measurements of the Energy Spectrum and Charge Composition of the Anomalous Components in 1977-1981," W. R. Webber and A. C. Cummings, Solar Wind 5 conference (1982).

A discussion of some of the work on the anomalous component is presented below:

Temporal Variations of the Anomalous Oxygen Component

The anomalous component of cosmic rays refers to a group of elements (principally He, N, O, and Ne) in the energy range from ~5 to ~50 MeV/nuc which are overabundant when compared to solar system or galactic abundances. This component was discovered in 1972 and since then most studies have used rather long time averages, typically on the order of months, because of relatively low counting rates from the typical cosmic ray telescope. The four CRS telescopes on each of the two Voyager spacecraft, with their large collecting power, have now allowed us to look at the anomalous oxygen rates with finer time resolution for the first time. We have examined the period from launch in late 1977 to the end of 1981 and we find several time periods where large recurrent temporal variations are present, with an ~26 day periodicity. Variations in intensity by a factor of up to 10 are observed. We have investigated the origin of these variations by comparing the oxygen rates to rates of other particle types and by intercomparing the rates of the two Voyagers.

Two examples of these variations are shown in Figure 2 (a period in 1978) and Figure 3 (a period in 1980) along with similar but much smaller variations in the > 75 MeV proton rate. The amplitude of the proton variations is ~10-15%, whereas the variation in the oxygen rate is much larger with a peak to valley ratio of perhaps 10 to 1 for the largest peaks. The average spacing between the four large proton peaks in Figure 3 is ~26 days, and there are apparently two such 26-day sequences in Figure 2. This timing and correlation suggest that the origin of the oxygen increases may be the same as the process responsible for the high energy proton variations. We have investigated this possibility by comparing the radial gradients of the two

particle populations. The large scale radial gradients for the anomalous oxygen and the >75 MeV protons have been previously reported by others for the 1 - 20 AU range by comparing the intensities at the Pioneer spacecraft to those near Earth. By using the separation of the two Voyager spacecraft we can determine the local radial gradients during the time intervals of the variations and compare these to the large scale gradients. In the 1978 period the spacecraft are ~4 AU from the Sun and ~0.3 AU apart. In 1980 they have moved out to an average radial position of ~7.2 AU and have moved apart ~ 1.25 AU. They are well aligned in both longitude and latitude. During the 1978 and 1980 time intervals Voyager 1 is always farther from the Sun than Voyager 2; thus for positive radial gradients Voyager 1 will measure a higher intensity than Voyager 2.

Figure 2

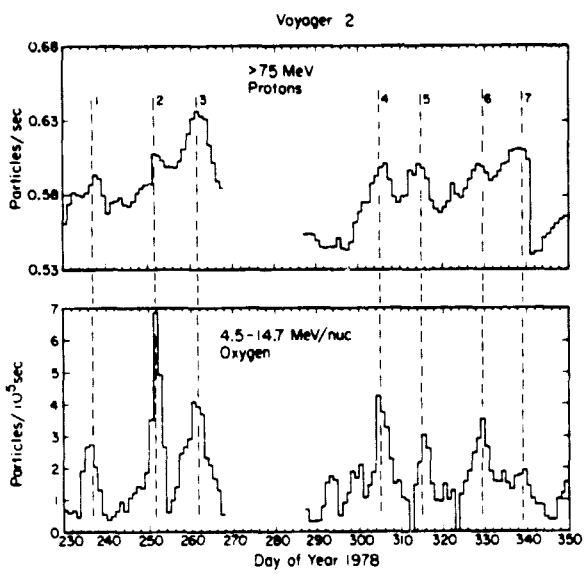

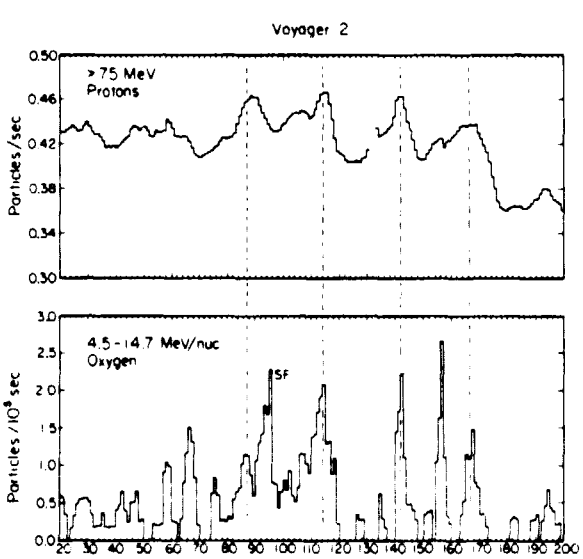

Figure 3

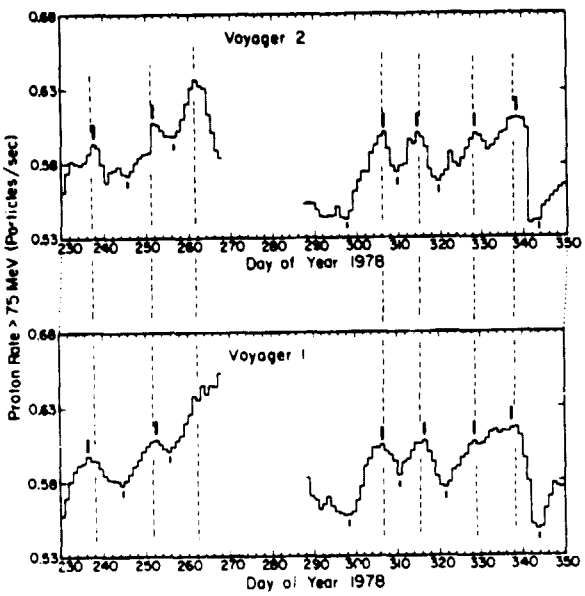

Figure 4

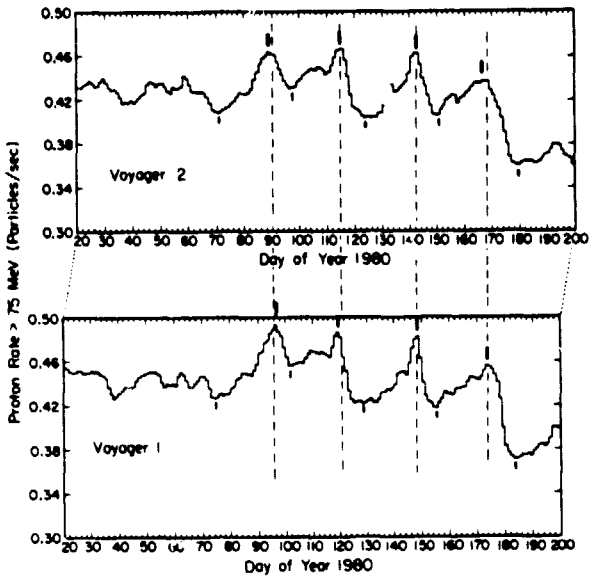

Figure 5

The comparison of the Voyager 1 and 2 proton rates for the 1978 period is shown in Figure 4. The correlation of features in the two plots is generally good. The corresponding plot for the 1980 period is shown in Figure 5. The corotation delay is ~6 days for this time interval and, after making the time shift, the features in the two panels line up well. We have taken the ratio of the Voyager 1 to Voyager 2 intensities for the correlated maxima and minima of the variations at the times indicated by the long and short vertical bars. The intensity ratios corresponding to the data in Figures 4 and 5 are shown in Figure 6 as a function of average radial distance from the Sun as the points near 4 AU for 1978 and near 7.2 AU for 1980. The lower panel of Figure 6 shows the ratio for the peak times and the upper panel shows the ratios for the times between the peaks. The remaining points near 6.4 AU are for a 1979 period when variations were also observed. The dashed lines on both panels show the computed intensity ratio for a given local radial gradient. It is apparent that the data from both panels are consistent with a local radial gradient of ~3 - 5%/AU which is consistent with the large scale gradients found for these particles from the Pioneer and near-Earth observations. These data therefore support the notion that the variations in intensity of the protons are due to a local modulation effect, most likely produced by a corotating magnetic field structure.

The Voyager 1 and 2 anomalous oxygen rate comparisons for the 1978 period are shown in Figure 7. The dashed lines indicate times of maximum proton fluxes from Figure 4. We could not duplicate the analysis procedure we used for the protons because of poorer statistics. Therefore we have summed over the time intervals shown by the horizontal bars to get a single ratio for the periods between the maxima of the proton fluxes. We have also summed over the seven 3-day periods associated with the proton flux maxima in order to calculate a single average ratio for the "peak" times. These values are shown in the second column of Table 1. The V1 to V2 ratio for the times between the peaks is within 1σ of the expected ratio of 1.05 for the large scale positive radial gradient of ~15%/AU which has been reported for

anomalous oxygen from Pioneer and near-Earth data. The ratio for the sum of the seven peaks is ~1.8σ less than 1.05. For comparison the third column of Table 1 shows the average V1 to V2 ratios for the high energy protons in 1978 as computed from the weighted average of the points shown in Figure 6. Ratios for both the peak and between-peak fluxes are consistent with the expected ratio for a radial gradient of 3 - 5%/AU.

TABLE 1. Ratios of V1 to V2 Intensity

	1978		1980	
	Anomalous oxygen	>75 MeV protons	Anomalous oxygen	>75 MeV protons
Periods of minimum proton flux	1.23 ± .18	1.013 ± .004	1.04 ± .25	1.041 ± .003
Periods of maximum proton flux	0.82 ± .13	1.006 ± .003	0.58 ± .17	1.047 ± .004
Expected for 15%/AU	1.05	---	1.20	---
Expected for 3 - 5%/AU	---	1.009 - 1.015	---	1.038 - 1.065
Average radial position	~ 4 AU		~ 7.2 AU	
Average radial separation	~ 0.3 AU		~ 1.25 AU	

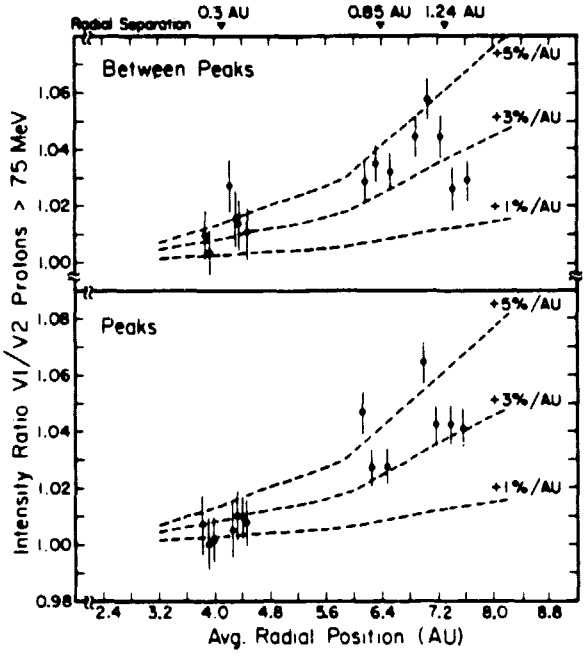

Figure 6

In Figure 8 we show the anomalous oxygen rate comparisons for 1980. The correlation of features in the Voyager 1 and 2 plots is less clear. We have made a relative shift of 6 days in the two plots just as we did for the protons, and the times of the four major proton peaks are shown by dashed lines and used as a guide in identifying the correlated peaks. The 3-day periods indicated by the vertical bars were summed to get an average ratio for the peak periods. The times indicated by horizontal bars were summed to calculate a between-peak period ratio. This division of time periods is less obvious in 1980 than in 1978. For example, there appear to be additional peak fluxes in oxygen between the times associated with proton flux maxima, particularly near day 157 in Voyager 2 and near day 108 in Voyager 1. In fact there may well be a second sequence of peaks offset from the primary sequence by ~10 days. A 5-day data gap from day 130-135 on Voyager 2 possibly obscures one of the peaks in the secondary sequence. The V1 to V2 ratios of the anomalous oxygen intensity for the two time periods are shown in the fourth column of Table 1. Here again the ratio for the times between the proton peaks is within 1σ of the expected ratio of 1.2. However, the ratio for the sum of oxygen fluxes during periods associated with proton flux maxima is ~3.7σ less than expected for a gradient of +15%/AU. The average proton intensity ratios, shown in the fifth column of Table 1, are again consistent with a 3 - 5%/AU radial gradient.

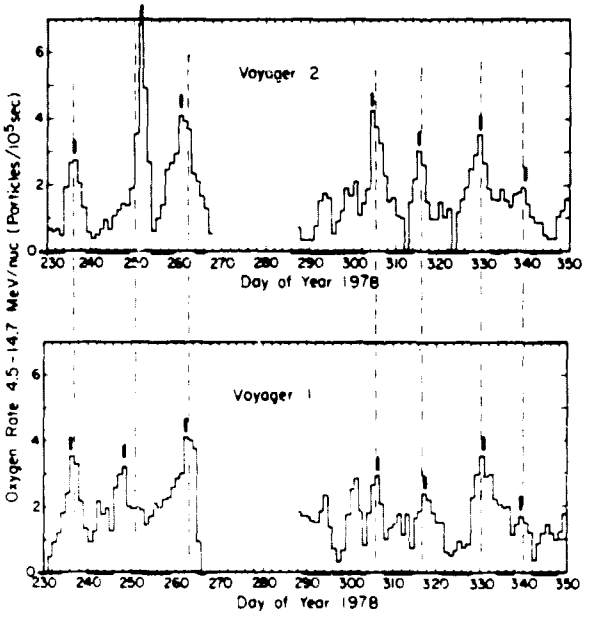

Figure 7

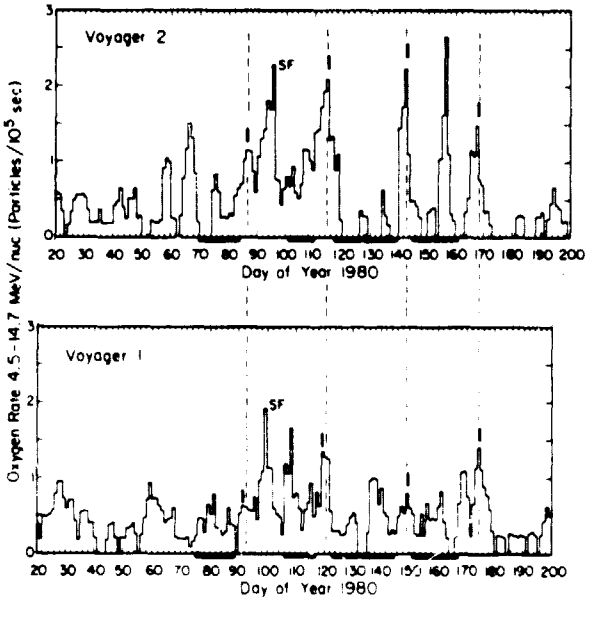

Figure 8

As we have noted, the >75 MeV proton variations appear to be small (~10-15%) perturbations on a rate which is well correlated over the separation distance of the two spacecraft. The local gradient derived for both the maxima and minima of the variations are consistent with the large scale gradients reported for separation distances of up to 20 AU. The oxygen variations, on the other hand, do not fit a similar picture. Particularly in 1980 (see Figure 8) when the spacecraft are ~1.25 AU apart, the features in the two rates are not well correlated; the peaks in Voyager 2 appear to be sharper and more well defined than in Voyager 1, the perturbations on the rate are not small, and the apparent local radial gradients for the peaks do not agree with

the overall large scale gradients that have been reported. The oxygen intensity variations appear to be more filamentary in nature than those of the protons, suggesting perhaps that the oxygen nuclei are more sensitive to the detailed configuration of the magnetic field than are the protons. These differences suggest that the origin of the short term oxygen variations is different from that of the protons.

1.2.3. A Heavy Isotope Spectrometer Telescope (HIST) Launched on ISEE-3 in August 1978

HIST is designed to measure the isotope abundances and energy spectra of solar and galactic cosmic rays for all elements from lithium to nickel ($3 \leq Z \leq 28$) over an energy range from several MeV/nucleon to several hundred MeV/nucleon. Such measurements are of importance to the study of the isotopic constitution of solar matter and of cosmic ray sources, the study of nucleosynthesis, questions of solar-system origin, studies of acceleration processes and studies of the life history of cosmic rays in the galaxy.

HIST was successfully launched on ISEE-3 and provided high resolution measurements of solar and galactic cosmic ray isotopes until December 1978, when a component failure reduced its isotope resolution capability. Since that time, the instrument has been operating as an element spectrometer for solar flare and interplanetary particle studies.

During the past year J. D. Spalding completed his Ph.D. thesis on the isotopic composition of heavy nuclei observed during the 9/23/78 solar flare. This study, and our work on galactic cosmic ray isotopes, has resulted in the following recent talks and papers.

- "Isotopic Studies of Heavy Nuclei in the 9/23/78 Solar Flare Event," R. A. Mewaldt et al., *Bull. Am. Phys. Soc.* **27**, 571 (1982).

- "Samples of the Milky Way," R. A. Mewaldt et al., *Scientific American* **247**, 100-109 (1982).

- "Isotopic Anomalies in Galactic Cosmic Rays," R. A. Mewaldt, *Bull. Am. Astron. Soc.* **14**, 645 (1982).

- "The Elemental and Isotopic Composition of Galactic Cosmic Ray Nuclei," R. A. Mewaldt, *Rev. Geophys. Space Phys.* (1983 in press).

- "The Isotopic Composition of Energetic Particles Emitted from a Large Solar Flare," J. D. Spalding, Ph.D Thesis, California Institute of Technology (1982).

A summary of some of the work in J. D. Spalding's Ph.D. thesis is given below:

<u>The Isotopic Composition of Energetic Particles Emitted from a Large Solar Flare</u>

Knowledge of the solar system isotope composition is essential to studies of the origin of the elements in stars, and studies of the solar system formation. Satellite-borne spectrometers which measure solar energetic particles (SEPs) now provide a new means of sampling directly the composition of solar material. Among the first results from HIST were high-resolution measurements of the isotopic composition of

Ne and Mg observed during the 9/23/78 solar flare. One surprising result of this work was that the $^{22}Ne/^{20}Ne$ ratio in this flare was significantly greater than that observed in the solar wind (SW). In his doctoral thesis, J. D. Spalding has determined the isotopic composition of additional elements (He, C, N, and O); studied the time and energy dependence of the isotopic composition; determined the elemental composition and spectral characteristics of this event; and obtained a more accurate value for $^{22}Ne/^{20}Ne$ in this flare, based on the analysis of additional data. Although the composition of C, N, O, and Mg isotopes is found to be consistent with terrestrial and meteoritic measurements, there continues to be a significant difference between the $^{22}Ne/^{20}Ne$ ratio in this flare and that for the solar wind. This difference is presently not understood, although there is also evidence for it from lunar and meteoritic studies of solar energetic particles.

The HIST telescope consists of a stack of silicon solid-state detectors, labeled M1, M2, and D1 through D9, in which the nuclear charge, mass, and kinetic energy of stopping nuclei is determined by conventional ΔE by E' techniques. Figure 9 shows mass histograms for 300 Ne events, more than double the previous sample. For convenience, the "Range" of particles stopping in HIST is labeled by the last detector triggered. The earlier HIST Ne measurement was based on Range 2 and Range 3 data. The bulk of the new data is at lower energy (Range 1), where the two position-sensitive detectors (M1 and M2) are used as ΔE devices. Although the Range 1 mass resolution (0.27 amu) is not expected to be as good as at higher energies (0.20 amu), there is a well-defined ^{22}Ne peak.

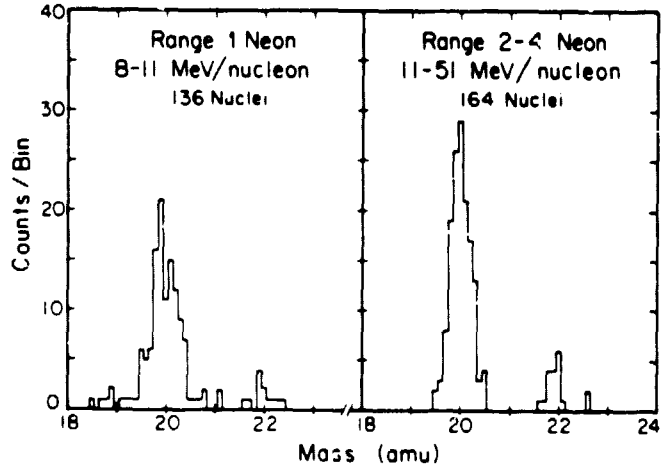

Figure 9

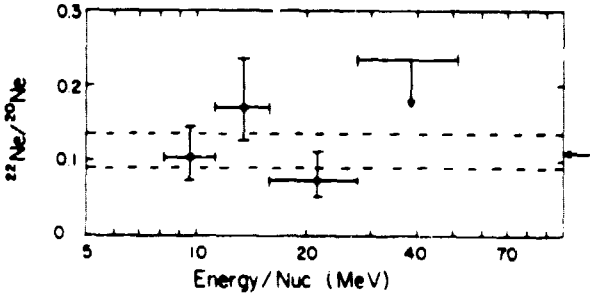

Figure 10

Figure 10 shows the $^{22}Ne/^{20}Ne$ ratio in four energy intervals. Although it is possible that this ratio may vary with energy, there is no obvious trend. Similarly, there is no evidence for any significant variation in the $^{13}C/^{12}C$, $^{18}O/^{16}O$, $^{25}Mg/^{24}Mg$, or $^{26}Mg/^{24}Mg$ ratios with energy, nor is there any significant time dependence for the isotopic composition during this solar event. In addition, the abundant elements from C to Si all have a similar spectral shape, with a relative composition consistent with other large solar events. There is, therefore, no evidence to suggest that this event would have an anomalous isotopic composition.

Table 2 summarizes the isotopic results obtained from HIST for six elements. The C, N, and O measurements represent the first isotopic studies of these elements in SEPs. The improved $^{22}Ne/^{20}Ne$ measurement is somewhat smaller but consistent with our earlier value of 0.13 (+.04, -.03). Also included is an improved upper limit for $^{21}Ne/^{20}Ne$, and an upper limit for $^{3}He/^{4}He$ in this event. In Figure 11 these results are compared with tabulated solar system abundances, SW measurements, and other SEP measurements. Note that in all cases the measured SEP ratios are consistent with Cameron's tabulation. However, it should be pointed out that the Cameron abundances are based primarily on measurements of terrestrial and meteoritic samples, and little is known about the extent to which they represent the composition of the Sun. This is especially true in the case of Ne, where, for example, the recent Anders and Ebihara table of solar system abundances uses the SW value ($^{22}Ne/^{20}Ne$ = 0.073) rather than the meteoritic component Neon-A ($^{22}Ne/^{20}Ne$ = 0.122), which Cameron chooses.

Table 2 - Isotope Ratios
9/23/78 Solar Flare

Isotope Ratio	Energy (MeV/nuc)	Observed Ratio[+]	Solar System[5]
$^{3}He/^{4}He$	5-32	< 0.0076	
$^{13}C/^{12}C$	6-39	$0.0095^{+.0042}_{-.0029}$	0.0112
$^{14}C/^{12}C$	6-39	< 0.0014	radioactive
$^{15}N/^{14}N$	9-47	$0.008^{+.010}_{-.005}$	0.0037
$^{17}O/^{16}O$	7-45	< 0.0021	0.00037
$^{18}O/^{16}O$	7-45	$0.0015^{+.0011}_{-.0007}$	0.00204
$^{21}Ne/^{20}Ne$	11-51	< 0.014	0.0030
$^{22}Ne/^{20}Ne$	8-51	$0.109^{+.026}_{-.019}$	0.122
$^{25}Mg/^{24}Mg$	12-36	$0.148^{+.043}_{-.025}$	0.129
$^{26}Mg/^{24}Mg$	12-36	$0.148^{+.046}_{-.026}$	0.142

[+]68% confidence intervals or 86% confidence limits

In Figure 12, selected solar system measurements of $^{22}Ne/^{20}Ne$ are shown on an expanded scale. Included, in addition to the meteoritic components neon-A and neon-B, is a third component, "neon-C", thought to represent SEP neon (≥ 1 MeV/nuc) directly implanted in lunar and meteoritic material. It is interesting that all of the attempts to measure this component find a $^{22}Ne/^{20}Ne$ ratio greater than that of present day SW Ne, and with one possible exception, greater than that of Neon-B, thought to represent implanted SW. In a recent review of these measure-

ments, Black concludes that neon-C has $^{22}Ne/^{20}Ne$ ratio of 0.090 to 0.097. Note that neither of the two satellite measurements could be considered inconsistent with this range.

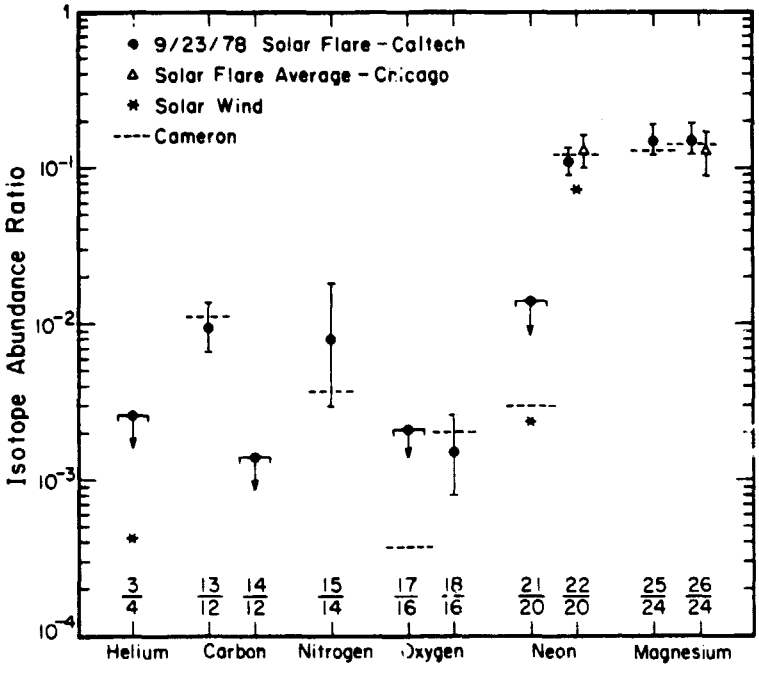

Figure 11

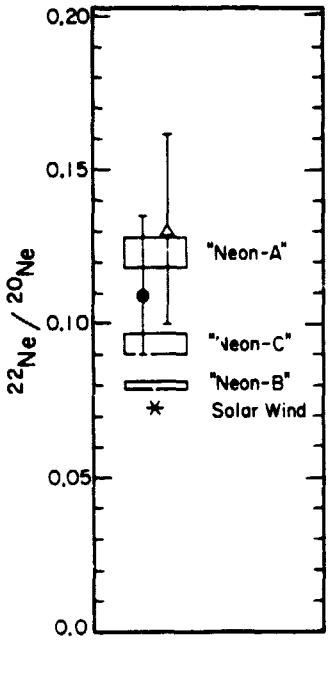

Figure 12

Thus, there a. two ndependent approaches that find a difference between SEP and SW neon. The questions remain as to how the Sun can apparently emit two distinct isotopic components, and which, if either, represents the composition of the Sun. We have considered the possibility of linear, mass-dependent fractionation, operating in either the solar flare acceleration or propagation processes, but find no evidence for such a pattern in our C, O, and Mg results. Although relatively little is known about the SW isotopic composition, neither does it appear that the SW isotopes have been altered by a simple mass-dependent fractionation process.

There are also models that might produce selective enhancements. Fisk's model for "^{3}He-rich" events can also enhance certain heavier elements. It is not clear, however, that it could produce isolated enhancements of individual heavy isotopes such as ^{22}Ne. Furthermore, there does not appear to be either a ^{3}He enhancement or an anomalous elemental composition in the 9/23/78 flare (our $^3He/^4He$ upper limit appears to be the lowest yet reported for a single solar event), suggesting that the conditions necessary for this model do not apply to this event. Mullen has proposed a pre-acceleration model that, on the average, would be expected to enhance the $^{22}Ne/^{20}Ne$ ratio more than other isotopic ratios. A test of this model, not yet possible with the present data, would be correlated enhancements of $^{22}Ne/^{20}Ne$ and $^{13}C/^{12}C$. It appears that comprehensive measurements of a number of isotopic ratios in both the SW and in a number of SEP events may be required to relate the SW and SEP isotopic composition to that of the Sun.

1.2.4. A Heavy Nuclei Experiment (HNE) Launched on HEAO-C in September 1979

The Heavy Nuclei Experiment is a joint experiment involving this group and M. H. Israel, J. Klarmann, W. R. Binns (Washington University) and C. J. Waddington (University of Minnesota). HNE is designed to measure the elemental abundances of relativistic high-Z cosmic ray nuclei ($17 \leq Z \leq 130$). The results of such measurements are of significance to the studies of nucleosynthesis and stellar structures, the existence of extreme transuranic nuclei, the origin of cosmic rays, and the physical properties of the interstellar medium. HNE was successfully launched on HEAO-3 and operated until the spacecraft gyro's failed in late May 1981.

A paper dealing with the ratio of the s-process elements $_{50}$Sn and $_{56}$Ba to the r-process elements $_{52}$Te and $_{54}$Xe is in press. This paper will show that this charge region, like the 30-42 region and the actinides, is not dominated by r-process nuclei. A more detailed analysis of this result will be the topic of a doctoral thesis by K. E. Krombel.

A prototype of the HEAO HNE was calibrated at the Lawrence Berkeley Lab Bevalac in November. Data were acquired with beams of $_{25}$Mn and $_{79}$Au. The Au beam was the first ultra-heavy beam transported down the external beam line. Analysis of the gold data for deviations from the usual assumption of Z^2 scaling is in progress at CIT.

The following talks and papers have been presented recently:

- "The Abundance of the Actinides in the Cosmic Radiation as Measured on HEAO-3," W. R. Binns et al., *Ap. J. (Lett.)* **261**, L117-L120 (1982).

- "Abundances of Cosmic Ray Sn, Te, Xe, and Ba Nuclei," E. C. Stone et al., *Bull. Am. Phys. Soc.* **27**, 534 (1982).

- "The Abundance of the Actinides in the Cosmic Radiation as Measured on HEAO-3," C. J. Waddington et al., *Bull. Am. Phys. Soc.* **27**, 534 (1982).

- "Secondary/Primary Ratios in Ultraheavy Cosmic Rays Measured on HEAO-3," W. R. Binns et al., *Bull. Am. Phys. Soc.* **27**, 534 (1982).

- "Cosmic Ray Abundances of Sn, Te, Xe, and Ba Nuclei Measured on HEAO 3," W. R. Binns et al., *Ap. J. (Lett.)* (1983 in press).

A résumé of the Sn-Ba study is presented below:

Cosmic-Ray Abundances of Sn, Te, Xe, and Ba Nuclei

The elements heavier than iron and nickel are assumed to have been formed primarily by neutron capture nucleosynthesis processes. These processes can be separated into two extreme classes depending on the intensity of the neutron flux involved. The r, or rapid, process, characterized by a high neutron flux, forms highly neutron-rich nuclei which decay back to the valley of beta stability only after the completion of nucleosynthesis. The s, or slow, process has a much lower flux of neutrons and allows for the decay of beta unstable nuclides before subsequent neutron captures. The r-process is usually associated with supernovae.

Both these processes produce a characteristic signature in the resulting elemental composition. These signatures are most evident in the relative abundances of $_{50}$Sn, $_{52}$Te, $_{54}$Xe, and $_{56}$Ba. The s-process produces a greater abundance of Sn and Ba; the r-process results in an overabundance of Te and Xe. In both processes odd charge elements are significantly less abundant.

HNE data, based on charges measured using Cerenkov signals of high energy nuclei, are shown in Figure 13. This measurement is the first to show resolved even element peaks in this charge region. Particles with charge between 49.0 and 59.0 have been superposed in the modulo 2 histogram in inset b. This procedure, which bins each particle according to the difference between its assigned charge and the nearest even integer, superposes the even (and odd) element charge peaks, thus allowing a statistically significant determination of the instrument resolution.

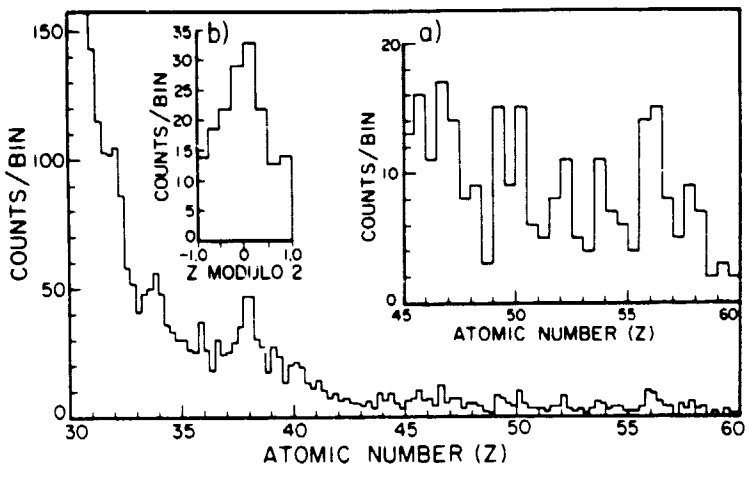

Figure 13

Figure 14 shows the derived abundances (points) compared to the calculations of N. Brewster using various sources. Since other results from lower charge regions indicate that there is an anticorrelation between first ionization potential and cosmic ray elemental abundances relative to the solar system the calculation has been done with and without adjustment for effects of first ionization potential (FIP). The data are not consistent with the assumed r-process source material in either case, but reasonable agreement is obtained with solar system source material adjusted for first ionization potential effects. Although the larg abundance of $_{58}$Ce shown in Figure 13 is also consistent with this conclusion, we have not considered it further here because its abundance is more affected by fragmentation of heavier nuclei.

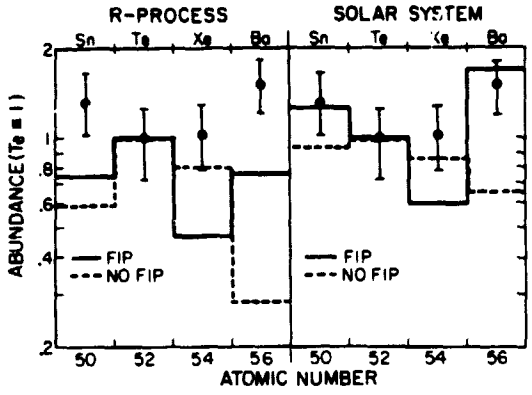

Figure 14

The large abundance of either Sn or Ba relative to the other elements in this group argue against a source dominated by the r-process. This conclusion is emphasized in Figure 15, which compares the ratio Sn/Te with the Ba/Te ratio. Our observed values are shown as the large diamond with 50% and 68% error ellipses. Also shown are various calculated values derived from several assumptions regarding the source composition. Points are plotted for pure r-process abundances, pure s-process abundances, and for solar system abundances, both with and without effects of first ionization potential. Two different predictions are shown (Brewster, Frier, and Waddington; and Blake and Margolis) to indicate the range of uncertainty in the calculations. Note that for a given propagation model and given assumptions about first ionization potential effects, the three calculated points fall on a straight "mixing line" whose ends represent pure r or pure s material, with varying r/s mixtures falling along the line.

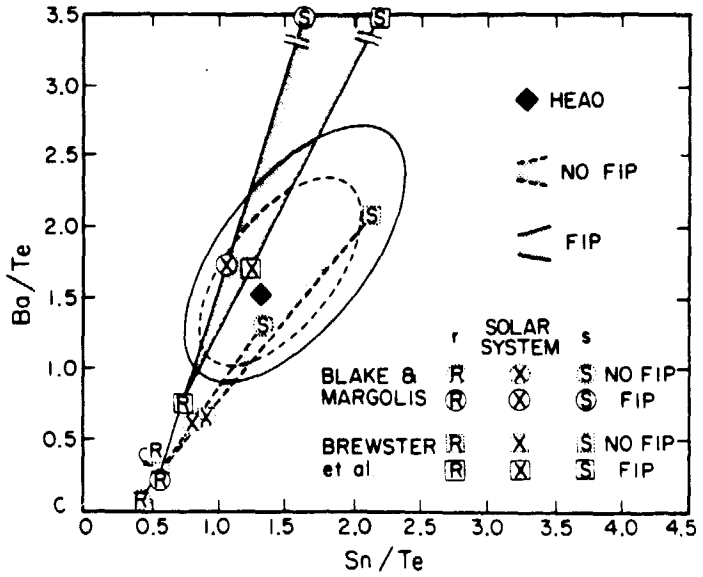

Figure 15

It is clear from this plot that our results are not consistent with pure r-process

material either with or without first ionization potential effects. The difference between the closest r-process point and our measurement is significant at the 93% level. When due account is taken of first ionization potential effects, our data are in reasonable agreement with solar system material whereas ignoring those effects suggests an s-process dominated mixture. The results in this charge interval are therefore consistent with our conclusions from measurements in other charge intervals since the measured elemental abundances in the charge 26 to 40 region show a similarity with solar system material adjusted for first ionization potential effects. Additionally the low abundance of the "actinides" (charges 88 to 100) is consistent with solar system material, but not with freshly synthesized pure r-process sources.

1.2.5. A Magnetometer Experiment on Pioneer 11

The Pioneer 11 Vector Helium Magnetometer Experiment is a joint investigation involving several research centers, with E. J. Smith (JPL) as Principal Investigator. Leverett Davis, Jr. (SRL) is the Caltech Coinvestigator on the experiment. A careful reanalysis of the magnetometer data taken within 8 Saturn radii has been made by Davis to obtain a spherical harmonic model. Careful exclusion of some questionable data, appropriate weighting of the data, and the use of the Singular Value Analysis codes of Lawson and Hanson yields a model that was substantially more accurate than the previous models. the most useful model is axisymmetric and uses a dipole, a quadrupole, and an octupole term for interior sources and a uniform axial field for the external sources. The fit is very good; the weighted r.m.s. residual being 1.8% of the r.m.s. field. This analysis shows that there are almost certainly very small non-axisymmetric terms but their inclusion does not significantly change any calculations based on the model. A paper presenting these results in is preparation.

Davis also worked as a co-author with J. E. P. Connerney and D. L. Chenette on a chapter in the prospective book on Saturn edited by T. Gehrels. The following article appeared in print during the reporting period:

- "An Analysis of the Structure of Saturn's Magnetic Field Using Charged Particle Absorption Signatures," D. L. Chenette and L. Davis, Jr., *J. Geophys. Res.* **87**, 5267-5274 (1982).

2. Gamma Rays

This research program is directed toward the investigation of galactic and solar gamma rays with spectrometers of high angular resolution and moderate energy resolution carried on spacecraft and balloons. The main efforts of the group, which are supported partially or fully by this grant, have been directed toward the following two categories of experiments.

2.1. Activities in Support of or in Preparation for Spacecraft Experiments

These activities generally embrace prototypes of experiments on existing or future NASA spacecraft and they complement and/or support such experiments.

2.1.1. A Balloon-Borne Gamma Ray Imaging Payload (GRIP)

The principal focus of our current gamma-ray astronomy effort is the construction of a balloon-borne imaging gamma-ray telescope for galactic and extragalactic astronomy observations. A shielded NaI Anger camera will be used in combination with a lead rotating coded aperture mask to achieve an imaging capability of 1000 0.6° pixels in a 20° field of view and a localization capability of 3 arc minutes for 10σ sources. This performance represents more than an order of magnitude improvement over previous balloon and satellite instrumentation. The 16"x2" NaI Anger camera plate will have an energy range of 30 keV to 3 MeV and achieve a continuum sensitivity of $6 \times 10^{-7} / cm^2 s keV$ at 1 MeV.

Figure 16 shows a drawing of the detector and coded aperture mask systems of the GRIP instrument.

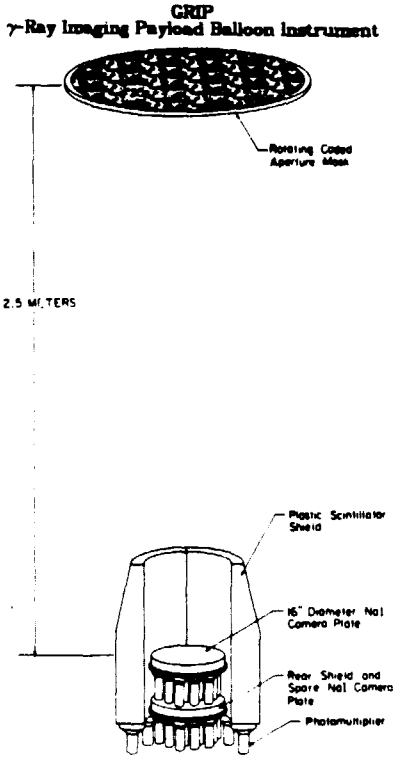

Figure 16

Considerable progress has been made during the last year in all principal hardware areas.

- Anger Camera: NaI crystal and 3" photomultiplier tubes procured. Initial tests of position response performed. Photomultipliers tested for dynamic range, linearity, and overload characteristics. Assembly of Anger camera system initiated.
- Shield System: NaI back shield and photomultipliers procured. Twelve plastic shield segments and photomultipliers procured and undergoing tests.
- Analog electronics: Prototype NaI signal processing chain designed, fabricated and tested.
- Pointing system, gondola, and mask: Mechanical design activity initiated.
- Data acquisition and image processing system: PDP 11/24 system procured includ-

ing disk drives, terminals, graphics printer, and storage CRT. UNIX operating system implemented and link established with SRL PDP 11/70 system for program development.

Table 3 lists the key parameters of the instrument.

Gamma-Ray Imaging Payload (GRIP) Balloon Experiment	
Primary Detector	40 cm x 5 cm NaI Anger Camera Position Resolution: 5 mm FWHM @ 200 keV
Shield	Back Plate: 5 cm NaI Side: 16 cm plastic scintillator Opening aperture: 48° FWHM
Mask	Hexagonal URA 1.1 m diameter x 2 cm Pb Spacing: 2.5 m from NaI detector Cell size: 2.5 cm No. of cells: 1750 Rotation rate: 1 rpm
Energy Range	0.03 - 3 MeV
Energy Resolution	8.3 keV @ 50 keV 78 keV @ 1 MeV
Sensitivity (2σ - 16 hr) (Brazil)	Continuum: ($\Delta E/E = 1$) @ 100 keV - 4×10^{-8} ph/cm^2 s keV @ 1 MeV - 6×10^{-7} ph/cm^2 s keV Broad Line: ($\Delta E/E$ = 1.2 x FWHM detector resolution) @ 100 keV - 2×10^{-4} ph/cm^2 s @ 0.511 MeV - 2×10^{-4} ph/cm^2 s @ 1 MeV - 2×10^{-4} ph/cm^2 s
Imaging	Resolution: 1000 0.6° diameter pixels Field of View: 20° Angular localization: 3 arc min (10σ source)

2.1.2. Gamma Ray Imaging Demonstration

During the last year we have performed a number of laboratory tests to demonstrate the capabilities of coded aperture imaging. Specifically, we have tested an imaging system consisting of a position sensitive NaI Anger camera and a rotating hexagonal uniformly redundant array (URA) mask. The tests were performed to gain experience with the imaging techniques to be used on the GRIP balloon experiment described earlier.

The hexagonal URA pattern is shown in Figure 17. It has a basic pattern of 127 cells which is repeated to give a total of approximately 1800 cells. The pattern has the advantageous feature that is very nearly antisymmetric under 60° rotation. This allows background subtraction to be performed at each detector position by a simple 60° rotation of the mask. Continuous rotation of the mask not only allows the position-by-position background subtraction just mentioned, but also allows the field of view to be extended without ambiguity by repetition of the basic URA pattern.

Figure 17

The coded aperture mask used in the laboratory tests was fabricated from 1 mm thick lead with a cell size of 1 cm. The Anger camera consisted of a 1/2" thick, 12" diameter NaI disk viewed by nineteen 2" photomultiplier tubes. A position resolution of 0.17 cm σ was achieved at 122 keV.

The laboratory test demonstrated the following imaging capabilities, which are illustrated in Figures 18-20:

- Imaging of point sources without artifacts by rotating hexagonal URA's.
- Extension of the field of view without ambiguity by utilizing mask rotation.
- Resolution of two nearby gamma-ray point sources

Figure 18 shows the image reconstruction of a point source using the rotating hexagonal URA mask. The information is displayed as a bar histogram with the height of each bar indicative of the measured source strength in a given direction. The point source is imaged without artifacts, and the point spread of the image agrees with predictions based on the position resolution of the Anger camera. This image utilizes only a single repetition of the basic URA pattern.

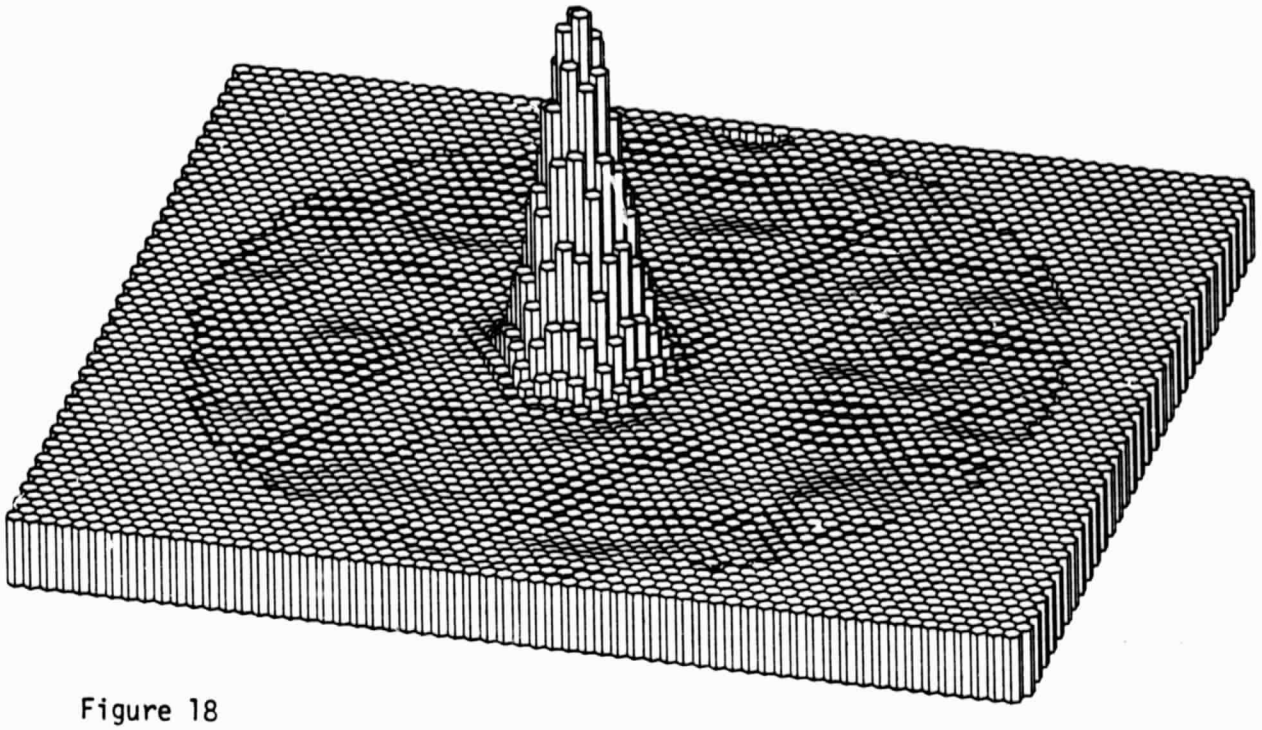

Figure 18

Figure 19a shows the image of a single gamma-ray point source obtained using the full coded aperture mask of Figure 17, but without rotation. It can be seen that there is a seven fold ambiguity in the source location. Figure 19b shows the effect of mask rotation in removing the ambiguity, thus allowing a sevenfold increase in the field of view. Note that the rotation leaves no other artifacts in the final image.

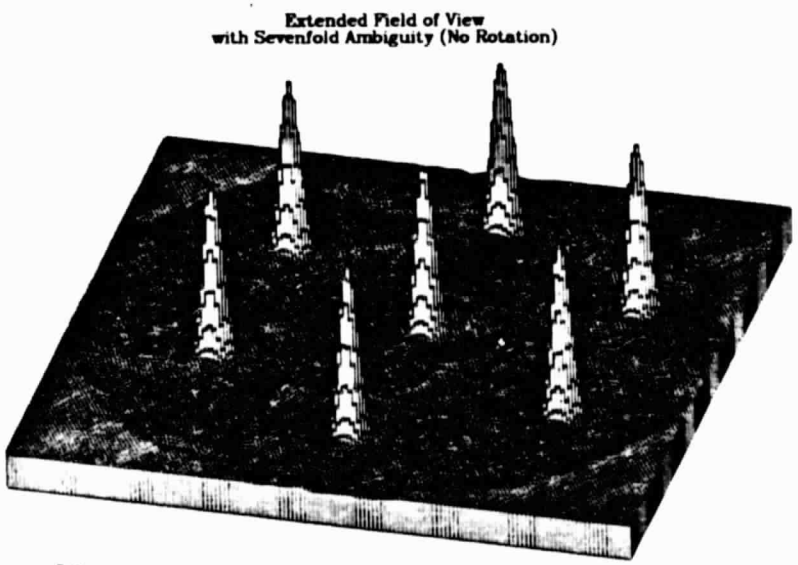

Figure 19a

Figure 19b

Figure 20 shows a grey scale and a peak image of two gamma-ray point sources, a strong (50σ) source and a weak (6σ) source. The sources are clearly resolved at an angular separation which corresponds to 1.1° for a 2.5 m mask-detector separation and a 2.5 cm cell size such as that to be used in the GRIP balloon instrument.

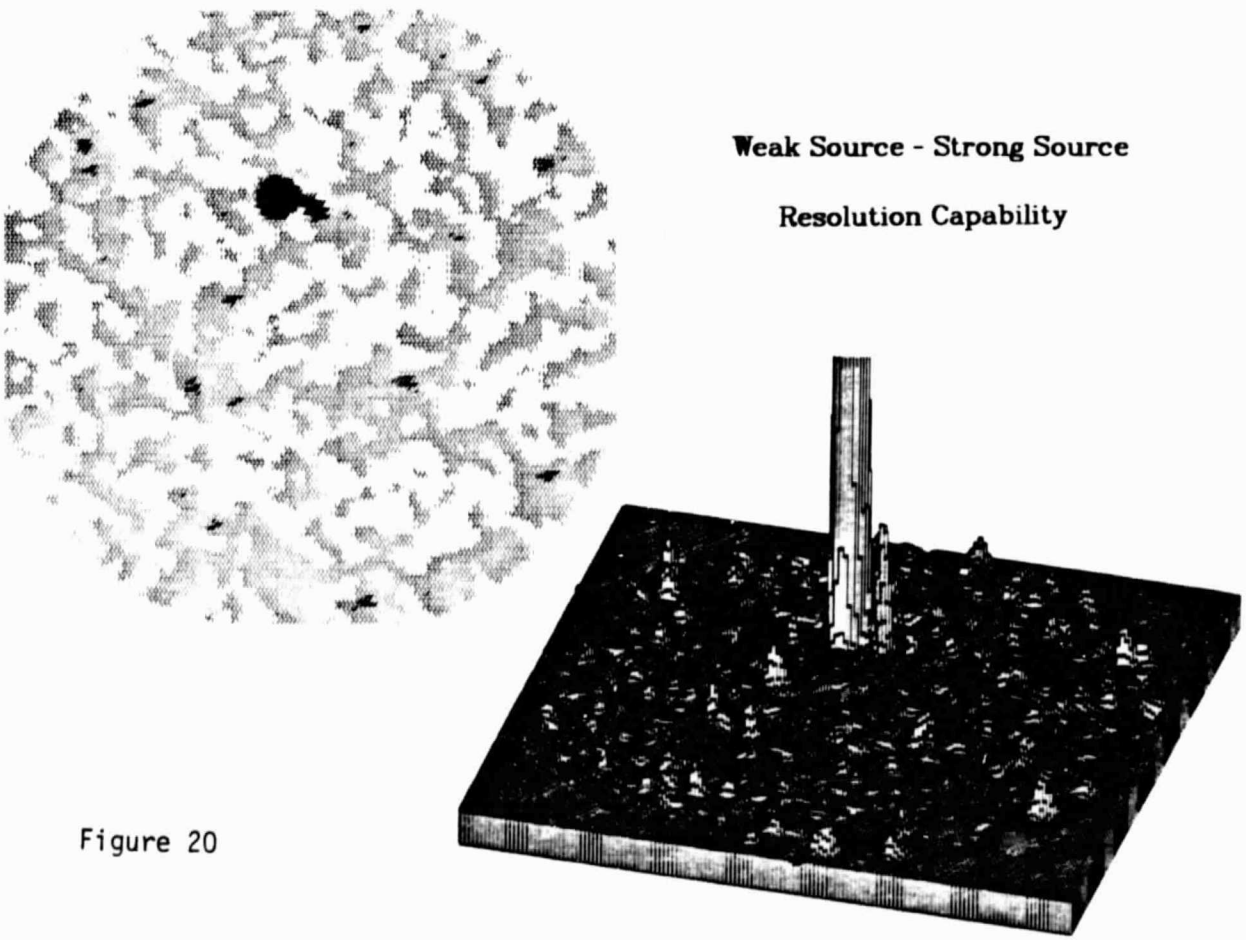

Figure 20

In summary, the laboratory tests of coded apertures have verified our expectations of their imaging capabilities. In particular, the analytical estimates for flux sensitivity, point source detection capability, angular resolution, and localization capability were all confirmed. The results indicate that an angular localization approaching 1 arc minute is feasible for balloon experiments together with a 1° resolution capability between neighboring sources. Future space experiments with much larger mask-detector spacings will achieve a localization capability of a few arc seconds together with an an angular resolution of a few arc minutes. In addition, the tests demonstrate that the use of rotating hexagonal URA's allows excellent position-by-position background subtraction as well as the extension of the field of view to large opening angles.

2.2. Experiments on NASA Spacecraft

2.2.1. A High Resolution Gamma-Ray Spectrometer on the HEAO-3 Spacecraft

The HEAO 3 spacecraft was launched in September, 1979. The primary mission of the HEAO 3 Gamma-Ray Spectrometer (GRS) is to make a complete survey of the sky with high energy resolution for sources of gamma-ray emission in the energy range 50 keV-10 MeV.

Data analysis activities on the HEAO-3 gamma-ray spectroscopy experiment in the past have included the 0.511 MeV galactic center positron annihilation line, the solar flare 2.22 MeV neutron capture line, and a search for nucleosynthesis lines from the Virgo cluster of galaxies. These activities were undertaken in collaboration with the High Energy Astrophysics Group of the Jet Propulsion Laboratory.

During the last year, the search for gamma-ray lines from the Virgo Cluster was completed. No lines were detected above a 3σ limit of 6×10^{-4} ph/cm^{2}s. Currently, activity on the HEAO-3 gamma-ray experiment involves an ongoing study of gamma-ray solar flare activity observed by HEAO-3 and participation in the data analysis meetings of the HEAO-3 team. These studies have resulted in the following papers.

- "Gamma-Ray and Optical Observation of the 1979 November 8 Solar Flare," G. R. Riegler et al., *Ap. J.* **259**, 392-396 (1982).

- "A High Resolution Measurement of the 2.223 MeV Neutron Capture Line in a Solar Flare," T. A. Prince et al., *Ap. J. (Lett.)* **255**, L81-L84 (1982).

2.2.2. The Gamma Ray Spectrometer Experiment on the Solar Maximum Mission (SMM)

The Solar Maximum Mission satellite was launched in early 1980 and has been in continuous operation observing gamma-ray emission from solar flares. The instrument is sensitive to photons in the energy range 0.3-100 MeV, and can also detect energetic neutrons above 40 MeV.

We have collaborated with the University of New Hampshire in the study of 2.22 MeV emission, following up on our earlier work with the HEAO-3 spacecraft. The focus of the SMM data analysis has been a study of 2.22 MeV line emission in a sample of 8 flares, which includes the very intense solar flare of 3 June 1982. The data from these flares have allowed a detailed study of the time history of the 2.22 MeV neutron

capture line from which conclusions have been drawn concerning the production of low energy neutrons in solar flares, the density at which neutrons are captured, and the ^{3}He abundance in the photosphere.

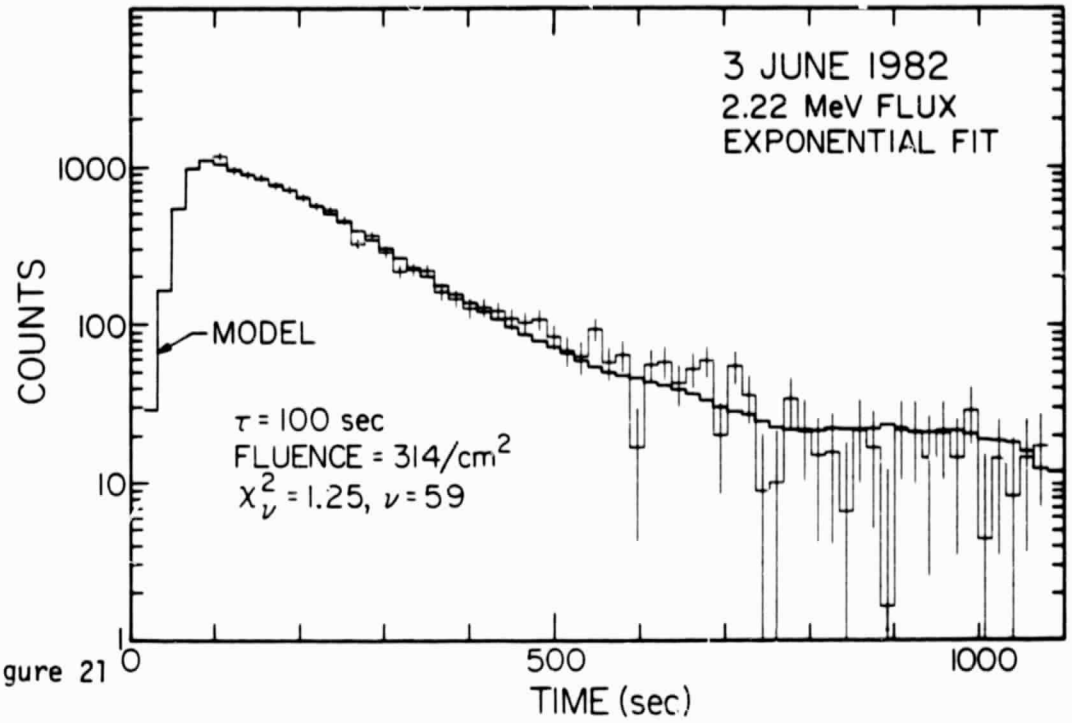

Figure 21

Figure 21 shows the time history of the 2.22 MeV emission from the 3 June 1982 flare together with a model fit assuming simple exponential decay following production of energetic neutrons in the impulsive phase of the flare. The time constant of the decay can be determined quite accurately from these data, namely τ=100 s. We are continuing our analysis of this particular flares and others from the SMM data set. This work has resulted in the following talk.

- "Comparison of 2.22 MeV Line Emission in Four Solar Flares," T. A. Prince et al., *Bull Am. Astron. Soc.* **14**, 875 (1982).

3. Other Activities

A. Buffington is serving as chairman of the APS Division of Cosmic Physics.

E. C. Stone continues to serve as NASA's Project Scientist for the Voyager Mission. He is also a member of the Space Science Board, the High Energy Astrophysics Management Operations Working Group, the Cosmic Ray Program Working Group, the Solar System Exploration Committee, and the NASA University Relations Study Group. He is currently a member of the Division for Planetary Sciences Committee of the American Astronomical Society.

T. A. Prince has been awarded Caltech's R. A. Millikan Fellowship for the two-year period 1981 and 1982.

4. Bibliography

Bieber, J. W., E. C. Stone, E. W. Hones, Jr., D. N. Baker, and S. J. Bame, "Plasma Behavior During Energetic Electrons Streaming Events: Further Evidence for Substorm Associated Magnetic Reconnection," *Geophys. Res. Ltrs.* 9, 664-667 (1982).

Bieber, J. W., E. C. Stone, E. W. Hones, Jr., E. N. Baker, S. J. Baker, S. J. Bame, and R. P. Lepping, "Reconnection - Associated Energization of Plasma Sheet Electrons," *EOS Trans. AGU* 63, 418 (1982).

Bieber, J. W., E. C. Stone, E. W. Hones, Jr., D. N. Baker, S. J. Bame, and R. P. Lepping, "Microstructure of Magnetic Reconnection in Earth's Magnetotail," *J. Geophys. Res.* (1983 submitted).

Binns, W. R., R. K. Fickle, T. L. Garrard, M. H. Israel, J. Klarmann, E. C. Stone, and C. J. Waddington, "The Abundance of the Actinides in the Cosmic Radiation as Measured on HEAO-3," *Ap. J. (Lett.)* 261, L117-L120 (1982).

Binns, W. R., R. K. Fickle, T. L. Garrard, M. H. Israel, J. Klarmann, E. C. Stone, and C. J. Waddington, "Secondary/Primary Ratios in Ultraheavy Cosmic Rays Measured on HEAO-3," *Bull. Am. Phys. Soc.* 27, 534 (1982).

Binns, W. R., R. K. Fickle, T. L. Garrard, M. H. Israel, J. Klarmann, K. E. Krombel , E. C. Stone, and C. J. Waddington, "Cosmic Ray Abundances of Sn, Te, Xe, and Ba Nuclei Measured on HEAO 3," *Ap. J. (Lett.)* (1983 in press).

Chenette, D. L. and L. Davis, Jr., "An Analysis of the Structure of Saturn's Magnetic Field Using Charged Particle Absorption Signatures," Talk presented at Tucson Saturn Conference, 1982, Tucson, Arizona.

Chenette, D. L., E. C. Stone, and R. E. Vogt, "The Companions of Mimas: Charged Particle Absorption Signatures and a Comparison with Recent Imaging Discoveries," Talk given at Tucson Saturn Conference, 1982, Tucson, Arizona.

Chenette, D. L. and L. Davis, Jr., "An Analysis of the Structure of Saturn's Magnetic Field Using Charged Particle Absorption Signatures," *J. Geophys. Res.* 87, 5267-5274 (1982).

Chenette, D. L. and E. C. Stone, "The Mimas Ghost Revisited: An Analysis of the Electron Flux and Electron Microsignatures Observed in the Vicinity of Mimas at Saturn," *J. Geophys. Res.* (1982 submitted).

Cummings, A. C. and W. R. Webber, "Temporal Variations of the Anomalous Oxygen Component," Solar Wind 5 conference (1982).

Gehrels, N. and E. C. Stone, "Energetic Oxygen and Sulfur in the Jovian Magnetosphere and Their Contribution to the Auroral Excitation," *J. Geophys. Res.* (1982 submitted).

Mewaldt, R. A., J. D. Spalding, and E. C. Stone, "Isotopic Studies of Heavy Nuclei in the 9/23/78 Solar Flare Event," *Bull. Am. Phys. Soc.* 27, 571 (1982).

Mewaldt, R. A., E. C. Stone, and M. E. Wiedenbeck, "Samples of the Milky Way," *Scientific American* 247, 100-109 (1982).

Mewaldt, R. A., "Isotopic Anomalies in Galactic Cosmic Rays," *Bull. Am. Astron. Soc.* **14**, 645 (1982).

Mewaldt, R. A., "The Elemental and Isotopic Composition of Galactic Cosmic Ray Nuclei," *Rev. Geophys. Space Phys.* (1983 in press).

Prince, T. A., J. C. Ling, W. A. Mahoney, G. R. Riegler, and A. S. Jacobson, "A High Resolution Measurement of the 2.223 MeV Neutron Capture Line in a Solar Flare," *Ap. J. (Lett.)* **255**, L81-L84 (1982).

Prince, T. A., D. J. Forrest, E. L. Chupp, G. Kanbach, and G. H. Share, "Comparison of 2.22 MeV Line Emission in Four Solar Flares," *Bull Am. Astron. Soc.* **14**, 875 (1982).

Riegler, G. R., J. C. Ling, W. A. Mahoney, T. A. Prince, W. A. Wheaton, J. B. Willett, H. Zirin, and A. S. Jacobson, "Gamma-Ray and Optical Observation of the 1979 November 6 Solar Flare," *Ap. J.* **259**, 392-396 (1982).

Spalding, J. D., "The Isotopic Composition of Energetic Particles Emitted from a Large Solar Flare," Ph.D Thesis, California Institute of Technology (1982).

Stone, E. C., "Voyager Observations of Saturn's Rings: An Overview," Invited talk presented at I.A.U, Colloquium No. 75, Toulouse, France.

Stone, E. C., "Voyager Observations of the Uranian Rings: A Preview," Invited talk presented at I.A.U, Colloquium No. 75, Toulouse, France.

Stone, E. C., "The Voyager Encounter with Uranus," pp. 275-291 in *Uranus and the Outer Planets*, ed. G. Hunt, Cambridge University Press, Cambridge, England (1982).

Stone, E. C., C. J. Waddington, W. R. Binns, R. K. Fickle, T. L. Garrard, M. H. Israel, J. Klarmann, and K. K. Krombel, "Abundances of Cosmic Ray Sn, Te, Xe, and Ba Nuclei," *Bull. Am. Phys. Soc.* **27**, 534 (1982).

Stone, E. C., "The Voyager Encounters with Saturn," *AIAA* (1983 submitted).

Waddington, C. J., W. R. Binns, R. K. Fickle, T. L. Garrard, M. H. Israel, J. Klarmann, and E. C. Stone, "The Abundance of the Actinides in the Cosmic Radiation as Measured on HEAO-3," *Bull. Am. Phys. Soc.* **27**, 534 (1982).

Webber, W. R. and A. C. Cummings, "Voyager Measurements of the Energy Spectrum and Charge Composition of the Anomalous Components in 1977-1981," Solar Wind 5 conference (1982).